



**HAL**  
open science

# Caractérisation du réflecteur sismique en contexte anisotrope

Nathalie Favretto-Cristini, Paul Cristini

► **To cite this version:**

Nathalie Favretto-Cristini, Paul Cristini. Caractérisation du réflecteur sismique en contexte anisotrope. CFM 2009 - 19ème Congrès Français de Mécanique, Aug 2009, Marseille, France. hal-03378645

**HAL Id: hal-03378645**

**<https://hal.science/hal-03378645v1>**

Submitted on 14 Oct 2021

**HAL** is a multi-disciplinary open access archive for the deposit and dissemination of scientific research documents, whether they are published or not. The documents may come from teaching and research institutions in France or abroad, or from public or private research centers.

L'archive ouverte pluridisciplinaire **HAL**, est destinée au dépôt et à la diffusion de documents scientifiques de niveau recherche, publiés ou non, émanant des établissements d'enseignement et de recherche français ou étrangers, des laboratoires publics ou privés.

# Caractérisation du réflecteur sismique en contexte isotrope

NATHALIE FAVRETTO-CRISTINI ET PAUL CRISTINI

Laboratoire de Mécanique et d'Acoustique, CNRS, 31 chemin J. Aiguier, 13402 Marseille Cedex 20, France

**Mots clefs :** Réflecteur, interface plane, interface courbe, zone de Fresnel à l'interface, onde réfléchi.

## Résumé :

*La région spatiale autour d'une interface, qui affecte réellement la réponse de cette interface, et donc le champ d'onde réfléchi, est d'intérêt majeur pour la caractérisation des réflecteurs sismiques et l'interprétation sismique basée sur les méthodes AVA. Nous montrons que pour des milieux homogènes élastiques et isotropes en contact, son extension latérale maximale correspond à la zone de Fresnel à l'interface, tandis que son extension verticale maximale peut quelquefois dépasser une longueur d'onde sismique. Pour un synclinal (respectivement, un anticlinal), cette région est plus grande (respectivement, plus petite) que celle décrite pour une interface plane.*

## Abstract :

*The spatial region in the vicinity of an interface which actually affects the interface response and, hence, the reflected wavefield is of particular interest for the characterization of reflectors from a seismic viewpoint and for seismic interpretation using AVA methodologies. We show that for homogeneous, isotropic, and elastic media its maximum lateral extent corresponds to the lateral extent of the Interface Fresnel zone, and that its maximum vertical extent may be sometimes greater than the seismic wavelengths. For a syncline (respectively, an anticline) the spatial region is larger (respectively, smaller) than described for a plane interface.*

## 1 Introduction

The basis of many seismic studies is the ray theory [1]. Nevertheless, as measured seismic data have a finite low-frequency content, it is accepted that seismic wave propagation is not limited to an infinitely narrow line called ray, but that it is extended to a finite volume of space around the ray path (i.e. the 1<sup>st</sup> Fresnel volume [1]) which contributes to the received wavefield for each frequency. The 1<sup>st</sup> Fresnel volume (hereafter, denoted FV) and its intersection with an interface, called the Interface Fresnel zone (IFZ), have received broad attention over past decades. These concepts are continually being developed and have found so many applications in seismology and in seismic exploration, that it is impossible here to review all the books and articles which pay attention to them in seismic wave propagation. Nevertheless, we shall mention the works of Červený and his co-authors compiled in [1].

Of particular interest are the size of the IFZ and the size of the volume of the reflector involved in reflection time measurements because each one can be related to the horizontal and vertical resolutions of seismic methods [2]. Until now, only the IFZ and the penetration depth of the FV below the interface have thus been considered in studies [3]. If seismic amplitudes at receivers have to be evaluated, the interface reflectivity must be determined. The underlying question is then : Considering an isolated interface, how thick are the spatial regions above and below the interface which may actually affect the interface response and, hence, the reflected wavefield ? To our knowledge, the spatial region above the plane interface in the incidence medium which also affects the interface response has never been identified. In addition, very few works are devoted to the computations of the IFZ at a curved interface. Moreover, most of them are mainly concerned with the case of normal wave incidence onto the interface [2].

We extend these studies to the case of the oblique wave incidence onto a spherically shaped interface of anticline or syncline type between two homogeneous, isotropic and elastic media. We derive analytical expressions for the size of the IFZ (i.e., the maximum lateral extent of the reflector volume). We also estimate analytically the maximum vertical extension of the volume which actually contributes to the seismic amplitude. Some illustrative results for a given medium configuration and for the three types of interface (e.g., plane, anticline and syncline) are presented. The influence of the wave incidence onto the interface, and the influence of the interface curvature, on the size of the reflector volume are more particularly investigated. In the remainder of the paper we assume that the interface of interest is isolated from all others. In addition, we only consider the P-P reflection.

## 2 Maximum lateral extent of a reflector

We consider two homogeneous isotropic elastic half-spaces in welded contact at a curved interface. The spherically shaped interface which can be of anticline or syncline type is tangent at the point  $M(0,0,z_M)$  to the plane  $z = z_M$  which will represent the plane interface of interest in our study. The  $xy$ -plane includes the point source  $S(-x_S,0,0)$  and the receiver  $R(x_S,0,0)$ . The vertical  $z$ -axis is directed downwards. A spherical wave with a constant amplitude is generated by the source in the upper half-space. The spherical wave can be decomposed into an infinite sum of plane waves (PW) synchronous with each other at the time origin. We consider the harmonic PW with the frequency  $f$  which propagates in the upper half-space with the velocity  $V_{P1}$  from  $S$  to  $R$ , after being reflected by the interface at the point  $M$  in a specular direction  $\theta$  with respect to the normal to the interface (Figure 1). Let the traveltime of the specular reflected wave be  $t_{SMR}$  which is the sum of the wave traveltime  $t_{SM}$  from the source  $S$  to the point  $M$  and the wave traveltime  $t_{MR}$  from the point  $M$  to the receiver  $R$ . The set of all possible rays  $SM_iR$  with constant traveltime  $t_{SMR}$  defines the isochrone for the source-receiver pair  $(S,R)$  relative to the specular reflection  $SMR$ . This isochrone describes an ellipsoid of revolution tangent to the interface at  $M$ , and whose rotational axis passes through  $S$  and  $R$ , defined by

$$\frac{x^2}{\left(\frac{z_M}{\cos\theta}\right)^2} + \frac{y^2 + z^2}{z_M^2} - 1 = 0 \quad . \quad (1)$$

This equation is valid whatever the curvature of the interface. The frequency-dependent spatial region which actually affects the reflected wavefield is known to be the 1<sup>st</sup> Fresnel volume (FV) corresponding to the pair  $(S,R)$  and associated with the wave reflection at  $M$ . By definition, the FV is formed by virtual diffraction points  $F$  such that the waves passing through these points interfere constructively with the specular reflected wave. This condition is fulfilled when the path-length difference is less than one-half of the wavelength  $\lambda_1 = \frac{V_{P1}}{f}$  corresponding to the dominant frequency  $f$  of the narrow-band source signal [1], or in other terms :

$$|t_{SF} + t_{FR} - (t_{SM} + t_{MR})| \leq \frac{1}{2f} \quad , \quad (2)$$

the quantity  $t_{XY}$  denotes the traveltime from  $X$  to  $Y$ . The FV is represented by only the part of the volume, bounded by two ellipsoids of revolution with foci at  $S$  and  $R$  which are tangent to fictitious planes parallel to the plane  $z = z_M$  and located at a distance  $\frac{\lambda_1}{4}$  below and above the plane  $z = z_M$  (Figure 1), which is situated above the interface of interest (e.g., plane, anticline, or syncline) in the upper half-space. The two ellipsoids of revolution are defined by

$$\frac{x^2}{\left(\frac{z_M}{\cos\theta} \pm \frac{\lambda_1}{4}\right)^2} + \frac{y^2 + z^2}{\left(\frac{z_M}{\cos\theta} \pm \frac{\lambda_1}{4}\right)^2 - z_M^2 \tan^2\theta} - 1 = 0 \quad . \quad (3)$$

The IFZ is defined as the extent of intersection of the FV by the interface which is here spherically shaped. Unlike the case of a plane interface, the IFZ is not represented by an ellipse centered at the reflection point  $M$  when the source  $S$  and the receiver  $R$  are situated at the same distance from the interface. Depending on whether the interface is of anticline or syncline type, the IFZ alters in shape appropriately and its size may not be determined in the same way for both types. The radius of the interface curvature  $R_{int}$  is considered positive if the interface appears convex to the incident wave. The radius  $R_{int}$  is then chosen positive for an anticline and negative for a syncline. The critical parameter is actually the ratio between the radius of curvature  $R_{iso}$  of the ellipsoid of revolution describing the isochrone for the pair  $(S,R)$  relative to the specular reflection  $SMR$  and the radius of the interface curvature  $R_{int}$ , the radius  $R_{iso}$  being equal to the depth  $z_M$  for normal wave incidence. Depending on whether this ratio is less or greater than unity, the size of the IFZ is defined as the extent of intersection of the ellipsoid of revolution located at the distance  $\frac{\lambda_1}{4}$  either above, or below the plane  $z = z_M$  by the syncline. On the contrary, the size of the IFZ for an anticline is defined as the extent of intersection of the ellipsoid of revolution located at the distance  $\frac{\lambda_1}{4}$  below the plane  $z = z_M$  by the anticline, whatever the value of its radius of curvature  $R_{int}$ . For the sake of brevity, we refer the reader to [4] for the complete derivation of the equations for determining the size of the IFZ for an anticline. We only present here the final results. The results relative to the syncline can be easily derived by replacing the (positive) radius of the anticline curvature  $R_{int}$  by the (negative) radius of the syncline curvature  $R_{int}$ .

For an anticline the maximum lateral semi-extent  $x_{max}$  of the IFZ following the  $x$ -axis in the  $xz$ -plane (i.e., in the plane of incidence) is defined by

$$x_{max} = a \left( 1 - \frac{z_{1,2}^2}{b^2} \right) \quad . \quad (4)$$

where  $a = \frac{z_M}{\cos\theta} + \frac{\lambda_1}{4}$  and  $b = (a^2 - z_M^2 \tan^2\theta)^{\frac{1}{2}}$ . The quantity  $z_{1,2} = \frac{z_M + R_{int} \pm \Delta^{\frac{1}{2}}}{1 - \frac{a^2}{b^2}}$ , where  $\Delta = (z_M + R_{int})^2 - \left(1 - \frac{a^2}{b^2}\right) [a^2 + z_M (z_M + 2R_{int})]$  is always positive, is chosen so that the inequality  $1 - \frac{z_{1,2}^2}{b^2} > 0$  is satisfied.

The maximum lateral semi-extent  $y_{max}$  of the IFZ following the  $y$ -axis in the  $yz$ -plane (i.e., in the direction perpendicular to the plane of incidence) is given by

$$y_{max} = \left\{ b^2 - \left[ z_M + \frac{\lambda_1}{4} \left( \frac{z_M}{\cos \theta} + \frac{\lambda_1}{8} \right) (z_M + R_{int})^{-1} \right]^2 \right\}^{\frac{1}{2}}, \quad (5)$$

where the quantity in the square root bracket is always positive. The characteristics  $x_{max}$  and  $y_{max}$  of the IFZ at the surface of the anticline depend on the position of the source-receiver pair, and also on the incidence angle  $\theta$  of the ray SM. Moreover, larger portions of the interface are involved for low-frequency than for high-frequency components of the wavefield. The characteristics  $x_{max}$  and  $y_{max}$  of the IFZ also depend on the radius of the interface curvature  $R_{int}$ . For sufficiently great radius  $R_{int}$ , the IFZ for the anticline is identical to the IFZ for the plane interface  $z = z_M$ . It is represented by an ellipse centered at the reflection point M whose in-plane semi-axis  $x_{max}$  and transverse semi-axis  $y_{max}$  are expressed as in [3].

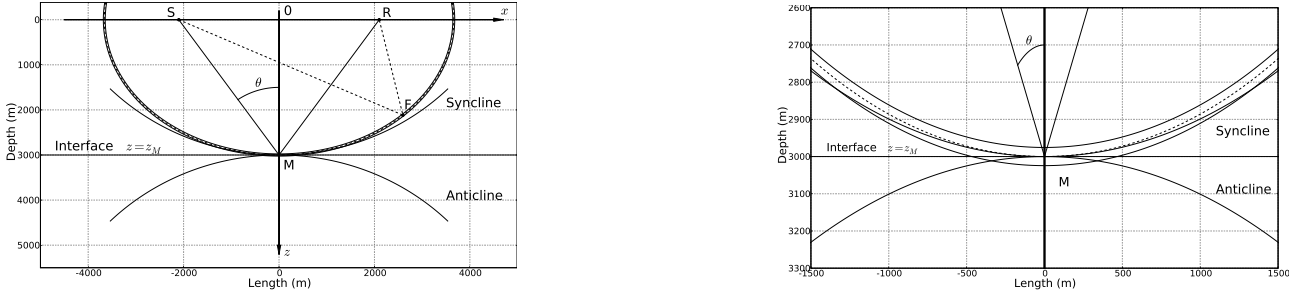


FIG. 1 – Representation, in the  $xz$ -plane, of the FV involved in the wave reflection at the point M at a curved interface of anticline or syncline type under the incidence angle  $\theta = 35^\circ$ . Left : The FV is given by the volume between the ellipsoids of revolution with foci at S and R and located in the upper half-space. Right : Focus on the FV in the vicinity of the interfaces. The dashed line describes the isochron for the source-receiver pair (S,R) relative to the specular reflection SMR.

### 3 Maximum vertical extent of a reflector

It is well-known that the FV of the reflected wave is not limited by the interface, but penetrates across the interface in the lower half-space. The penetration depth can be evaluated approximately in an analytical way following traveltime measurements or in a numerical way using the network ray tracing [1]. We proposed in [4] to derive analytically, in a straightforward manner, an approximate expression for the penetration depth of the FV across the curved interface, valid in the plane of symmetry between S and R and for subcritical incidence angles. By using the curvature transmission law and the concept of the fictitious source-receiver pair, we can obtain a new expression for the maximum penetration depth  $D_2$  in the lower half-space that provides more accurate results than those given in [3]

$$D_2 = \left( z_{S'}^2 + \frac{\lambda_2 z_{S'}}{2 \cos \theta'} + \frac{\lambda_2^2}{16} \right)^{\frac{1}{2}} - z_{S'} \quad (6)$$

with  $z_{S'} = \frac{z_M V_{P1} \cos^3 \theta'}{V_{P2} \cos^3 \theta + \frac{z_M}{R_{int}} (V_{P2} \cos \theta - V_{P1} \cos \theta')}$ , where  $V_{P2}$  denotes the velocity in the lower half-space and the transmission angle  $\theta'$  is connected to the incidence angle  $\theta$  through Snell's law. As this expression is evaluated locally in the plane of symmetry between S and R and for subcritical incidence angles  $\theta$ , it is valid whatever the radius of the interface curvature  $R_{int}$ . Expansion of equation 6 shows that for the values of the incidence angle  $\theta$  close to zero, and then for great position  $z_{S'}$ , the 1<sup>st</sup>-order approximation to penetration depth  $D_2$  with respect to  $\frac{1}{z_{S'}}$   $\left( \frac{\lambda_2 z_{S'}}{2 \cos \theta'} + \frac{\lambda_2^2}{8} \right)$  corresponds to the approximation given by equation 38 in [3].

Following the same reasoning, a region above the interface in the upper half-space also contributes to the interface response and, hence, to the reflected wavefield. The maximum thickness  $D_1$  of this region can be evaluated in the plane of symmetry between S and R and for subcritical incidence angles  $\theta$  in the same way as above

$$D_1 = \left( z_{S''}^2 + \frac{\lambda_1 z_{S''}}{2 \cos \theta} + \frac{\lambda_1^2}{16} \right)^{\frac{1}{2}} - z_{S''} \quad (7)$$

with  $z_{S''} = \frac{z_M R_{int} \cos^2 \theta}{2 z_M + R_{int} \cos^2 \theta}$ .

A reflector is therefore a volume of integration of the medium properties above and below the interface. Its maximum lateral extent corresponds to the lateral extent of the IFZ and its maximum vertical extent corresponds to the thickness  $D = D_1 + D_2$ . In this work we consider that the elastic media in contact are homogeneous and isotropic. The presence of heterogeneities or anisotropy in the media body may modify the size of the reflector volume. In addition to provide more physical insights into wave reflection process, our study may have significant implications on seismic interpretation using AVA methodologies. On one hand, when amplitude measurements are considered, we have to evaluate the interface reflectivity by considering the effective reflector volume which actually affects it, and by accounting for the heterogeneities located within. However, in the absence of heterogeneity located within the reflector volume, we only have to account for the IFZ for modeling the interface response. In previous works [5, 6], we have pointed out the consequences of ignoring the IFZ in forward and inverse modelings of seismic wave reflection. On the other hand, when only traveltime measurements are considered, for instance for locating the reflectors in the media, only the region below the interface with the thickness  $D_2$  has to be considered.

## 4 Results and discussion

In order to illustrate the theoretical derivations, two cases of curved interfaces and one case of plane interface between elastic half-spaces are chosen. The source-receiver plane is located at a distance  $z_M = 3000$  m from the plane tangent to the curved interfaces which can be of anticline or syncline type. The radius of the interface curvature  $R_{int}$  is equal to  $\pm 5000$  m. It is positive for an anticline and negative for a syncline. The plane  $z = z_M$  represents the plane interface of interest. The velocities of the upper and lower half-spaces are  $V_{P1} = 2000$  m/s and  $V_{P2} = 2800$  m/s, respectively. The frequency  $f$  being chosen is 25 Hz, and the seismic wavelengths in the upper and lower half-spaces are then  $\lambda_1 = 80$  m and  $\lambda_2 = 112$  m, respectively. The critical angle is equal to  $\theta_C = 45.58^\circ$ .

Figure 2 depicts the variation in the size of the IFZ for an anticline and a syncline as a function of the incidence angle  $\theta$ , for the given value of the radius of the interface curvature  $R_{int}$ . The variation in the size of the IFZ for a plane reflector is also shown for comparison. For  $\theta = 0$  and for a given type of interface, the in-plane semi-extent  $x_{max}$  and the transverse semi-extent  $y_{max}$  are equal. Following the type of interface, the IFZ is then represented either by a plane, or by a curved disk. With increasing  $\theta$  the IFZ becomes larger and larger in the incidence plane than in the transverse plane. This feature is more particularly pronounced for the syncline, the maximum size in the incidence plane being reached at a particular incidence angle  $\theta$  where the radius of the interface curvature  $R_{int}$  approaches the radius of curvature  $R_{iso}$  of the ellipsoid of revolution describing the isochrone for the source-receiver pair relative to the specular reflection SMR. This is more clearly shown in Figure 3 which depicts the variation in the size of the IFZ for an anticline and a syncline as a function of the radius of the interface curvature  $R_{int}$ , for a given incidence angle  $\theta$ . When the radius  $R_{iso}$  is greater than the threshold value leading to the maximum size of the IFZ in the incidence plane, the in-plane semi-extent  $x_{max}$  then decreases because the IFZ is no longer defined as the intersection of the ellipsoid of revolution located at the distance  $\frac{\lambda_1}{4}$  below the plane  $z = z_M$  by the syncline, but rather as the intersection of the ellipsoid located at the distance  $\frac{\lambda_1}{4}$  above the plane  $z = z_M$  by the syncline (Figure 1). As suggested above, the critical parameter is therefore the ratio between the radius  $R_{iso}$  and the radius  $R_{int}$ . We can easily show after straightforward calculations that for the syncline (respectively, anticline) the IFZ in the incidence plane is increased (respectively, decreased) in size, as compared to that for a plane interface, approximately by the factor

$$F_{S,A} = \left( 1 + \frac{z_M}{R_{int}} \frac{\beta^2}{\beta^2 - z_M^2 \tan^2 \theta} \right)^{-1}, \quad (8)$$

with negative (respectively, positive) radius  $R_{int}$  and  $\beta = \frac{z_M}{\cos \theta} \pm \frac{\lambda_1}{4}$ , the sign + (respectively, -) corresponding to the choice of the ellipsoid of revolution located at the distance  $\frac{\lambda_1}{4}$  below (respectively, above) the plane  $z = z_M$  (respectively,  $\beta = \frac{z_M}{\cos \theta} + \frac{\lambda_1}{4}$ ). The factors  $F_S$  and  $F_A$  tend to those given in [2] when the wave incidence is normal to the interface.

Similar conclusions can be drawn for the variation in the maximum semi-extent  $y_{max}$  of the IFZ in the transverse plane for the anticline and the syncline. The critical parameter which influences the length  $y_{max}$  is the ratio between the radius of curvature  $R_{iso}$  of the ellipsoid of revolution describing the isochrone for the source-receiver pair relative to the specular reflection SMR in the transverse plane (i.e. the depth  $z_M$  of the reflection point M) and the radius of the interface curvature  $R_{int}$ . For the anticline (respectively, the syncline) the IFZ in the transverse plane is decreased (respectively, increased) in size, as compared to that for a plane interface, approximately by the factor

$$F = \left( 1 + \frac{z_M}{R_{int}} \right)^{-1}, \quad (9)$$

with positive radius  $R_{int}$  for the anticline and negative radius  $R_{int}$  for the syncline. Note in Figure 3 that when the value of the radius of the interface curvature  $R_{int}$  tends to infinity the size of the IFZ for a curved interface

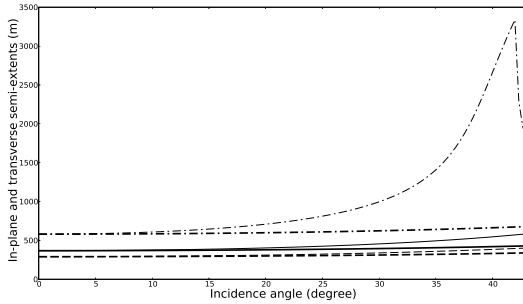


FIG. 2 – Variation in the size of the IFZ at the surface of an anticline (dashed line) and a syncline (dash-dot line), as a function of the incidence angle  $\theta$ , as compared with the results for a plane interface (solid line). Light curves are associated with the in-plane semi-extent  $x_{max}$ , while bold curves represent the variation in the transverse semi-extent  $y_{max}$ .

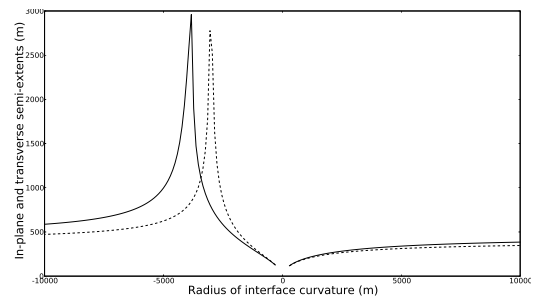


FIG. 3 – Variation in the in-plane semi-extent  $x_{max}$  (solid lines) and in the transverse semi-extent  $y_{max}$  (dashed lines) of the IFZ at the surface of an anticline (positive radius of interface curvature) and a syncline (negative radius of interface curvature), as a function of the radius of interface curvature  $R_{int}$ . The incidence angle  $\theta$  is equal to  $30^\circ$ .

tends to that for a plane interface.

Figure 4 shows the variation in the penetration depth  $D_2$  as a function of the incidence angle  $\theta$ , for the given value of the radius of the interface curvature  $R_{int}$  for the anticline and the syncline. It also presents the variation in the penetration depth  $D_2$  as a function of the incidence angle  $\theta$  for a plane interface. In order to check the accuracy of our approximation, the approximate results provided by equation 6 have been compared with the exact values [4] for the anticline and the syncline. For  $\theta = 0$ , the penetration depth  $D_2$  equals the well-known value  $\frac{\lambda_2}{4}$  [3], as for the plane interface. The penetration depth  $D_2$  increases with increasing subcritical angle  $\theta$ , but is always less than the seismic wavelength  $\lambda_2$ . For the syncline it can be greater than the seismic wavelength  $\lambda_1$  for subcritical incidence angles  $\theta$  close to the critical angle  $\theta_C = 45.58^\circ$ . Moreover, the values for the depth  $D_2$  provided by our approximation deviate only slightly from the exact values for the syncline, the discrepancies being less than 0.01 % up to the angle  $\theta = 43^\circ$  which is in the vicinity of the critical angle  $\theta_C$ . For the anticline the discrepancies between them do not exceed 0.01% up to the angle  $\theta = 40^\circ$  and 7.5% up to the angle  $\theta = 43^\circ$ , our approximation underestimating the exact value for the penetration  $D_2$ . Note that whatever the type of interface, the penetration depth  $D_2$  has the same values for incidence angle  $\theta$  lying between 0 and approximately  $30^\circ$ . For subcritical angles lying above  $30^\circ$  the penetration depth  $D_2$  for the syncline is, however, greater than that for the anticline. By comparing the curves obtained for the curved interfaces and those obtained for the plane interface, we can note that the penetration depth  $D_2$  for the syncline is increased in length, as compared to that for a plane interface, approximately by 16%, while the penetration depth  $D_2$  for the anticline is decreased approximately by 10%. Similar conclusions can be drawn for the case of a plane interface. The variations in the penetration depth  $D_2$  as a function of the incidence angle  $\theta$  provided by our approximation (equation 6), compared with the values obtained with the approximation of Kvasnička and Červený and with the exact values [4], are also shown in Figure 4. With increasing subcritical angle  $\theta$  the penetration depth  $D_2$  increases, but is always less than the seismic wavelength  $\lambda_2$ . Moreover, the values for  $D_2$  provided by our approximation deviate only slightly from the exact values. The discrepancies between them do not exceed 0.44% up to the angle  $\theta = 40^\circ$  and 4% up to the angle  $\theta = 43^\circ$  which is in the vicinity of the critical angle  $\theta_C = 45.58^\circ$ . On the contrary, the discrepancies between the values for  $D_2$  given by the approximation of Kvasnička and Červený and the exact solution strongly increase with increasing angle  $\theta$ , more particularly for angles above  $30^\circ$ . For  $\theta = 43^\circ$  the discrepancies exceed 23%. As a consequence, the part of a reflector below the interface which actually affects the interface response is smaller than described by previous estimates. This conclusion has been found to come true whatever the medium configuration chosen.

Figure 5 displays the variation in the thickness  $D_1$  above the interface in the upper half-space, as a function of the incidence angle  $\theta$ , for the given value of the radius of the interface curvature  $R_{int}$  for the anticline and the syncline. In order to check the accuracy of our approximation, the approximate results provided by equation 7 have been compared with the exact values [4]. The approximate values for  $D_1$  deviate only slightly from the exact values, the discrepancies between them lying below 0.05% up to the angle  $\theta = 43^\circ$ . Figure 5 also depicts the variation in the distance  $D_1$  as a function of the incidence angle  $\theta$ , for a plane interface. In this case, the distance  $D_1$  provided by equation 7 is evaluated exactly. Whatever the type of interface and for the normal wave incidence ( $\theta = 0$ ), the distance  $D_1$  equals the value  $\frac{\lambda_1}{4}$ . The thickness  $D_1$  increases with increasing incidence angles  $\theta$ , but is always less than both the seismic wavelength  $\lambda_1$  and the penetration depth  $D_2$ . Moreover, the thickness  $D_1$  is not much influenced by the interface curvature, the discrepancies between the curves associated with the syncline and the anticline being less than 1%.

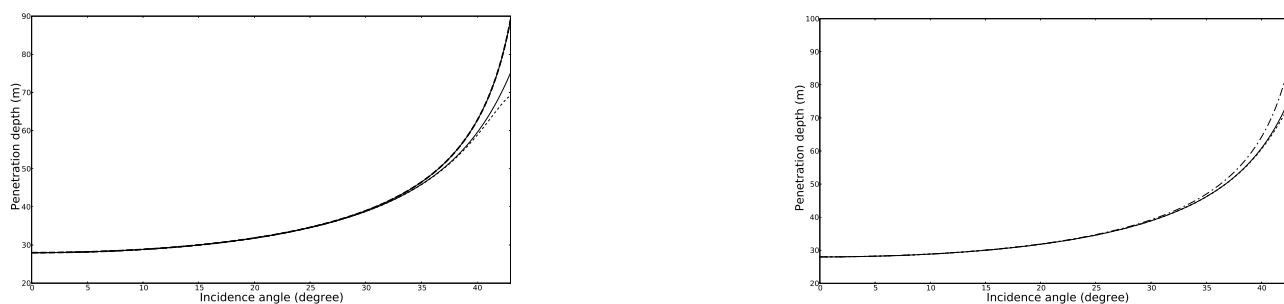


FIG. 4 – Variation in the penetration depth  $D_2$ , as a function of the incidence angle  $\theta$ , (left) for an interface of anticline (light curves) or syncline (bold curves) type. Comparison of results provided by our approximation (dashed lines) with the exact solution (solid lines); (right) for a plane interface. Comparison of results provided by our approximation (dashed line) with exact solution (solid line) and results predicted by the approximation of Kvasnička and Červený (dash-dot line).

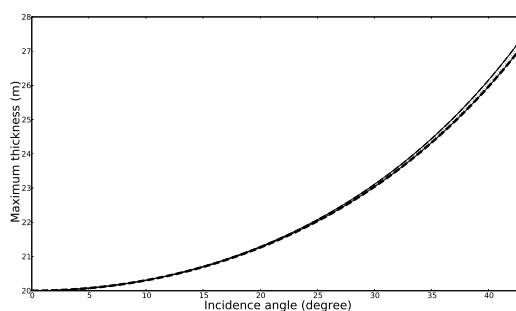


FIG. 5 – Variation in the maximum thickness  $D_1$  as a function of the incidence angle  $\theta$ , for an interface of anticline (light curves) or syncline (bold curves) type and for a plane interface (dotted line). Comparison of results provided by our approximation (dashed line) with the exact solution (solid line).

## Conclusion

We have identified the zone in the vicinity of a (plane or curved) interface which actually affects the interface reflectivity, and we have established the spatial limits of the effective reflector volume which merits further investigation. Although these spatial limits may vary following the complex properties of the bulk media in contact, defining these limits for homogeneous and isotropic media in contact enables us to fix ideas and to provide a road map for future applications to real media. For this case, the effective reflector volume has got its maximum lateral extent equal to the lateral extent of the IFZ, and its maximum vertical extent equal to a thickness which may be greater than the seismic wavelength of the incident wave for great incidence angles close to the critical angle.

## Acknowledgments

This work was supported in part by the Agence Nationale de la Recherche (ANR) under the EMSAPCO2 project.

## Références

- [1] Červený V. Seismic Ray Theory. Cambridge University Press, Cambridge, UK, 2001.
- [2] Lindsey J. The Fresnel zone and its interpretative significance. *The Leading Edge*, 8(10), 33–39, 1989.
- [3] Kvasnička M. and Červený V. Analytical expressions for Fresnel volumes and interface Fresnel zones of seismic body waves. Part 1 : Direct and unconverted reflected waves. *Studia Geophysica et Geodetica*, 40, 136–155, 1996.
- [4] Favretto-Cristini N., Cristini P., and de Bazelaire E. What is a seismic reflector like? *Geophysics*, 74(1), T13–T23, 2009.
- [5] Favretto-Cristini N., Cristini P., and de Bazelaire E. Influence on the Interface Fresnel zone on the reflected P-wave amplitude modelling. *Geophysical Journal International*, 171, 841–846, 2007.
- [6] Favretto-Cristini N., Cristini P., and de Bazelaire E. On the use of the interface fresnel zone concept for estimating media parameters from ava curves. In *Eighth International Conference on Theoretical Computational Acoustics Heraklion, Crete (Greece) 2-5 July, 2007*.